DOI:https://doi.org/10.15276/aait.03.2019.4
UDC 004.942:621.923

TEMPERATURE MODELS FOR GRINDING SYSTEM STATE MONITORING

Natalia V. Lishchenko[1)]
ORCID: https://orcid.org/0000-0002-4110-1321, odeslnv@gmail.com
Vasily P. Larshin[2)]
ORCID: https://orcid.org/0000-0001-7536-3859, vasilylarshin@gmail.com
[1)] Odessa National Academy of Food Technology, 112, Kanatnaya St. Odesa, 65039, Ukraine
[2)] Odessa National Polytechnic University, 1, Shevchenko Avenue. Odesa, 65044, Ukraine

ABSTRACT

The grinding temperature limits the productivity of this operation and is an important parameter for assessing the state of the grinding system. However, there is no information about the current grinding temperature in the existing computer systems for monitoring and process diagnostics on CNC grinding machines. This is due to the difficulty of measuring this parameter directly or indirectly. In the first case – difficulty with the installation of temperature sensors, in the second – there are no acceptable mathematical models for determining the grinding temperature. The objective of the study is development of a simpler temperature model which is acceptable for the modern grinding with large values of the workpiece velocity relative to the grinding wheel. To reach the study objective a classification of solutions of three-, two-, and one-dimensional differential equations of heat conduction with the same initial and boundary conditions was made to research the grinding temperatures with the help of these solutions under otherwise equal conditions. The conditions of results close agreement of the solutions are established depending on the geometrical configuration of the contact zone between the grinding wheel and the workpiece: H / L <1 and H >4, where H and L are half width and half length of the contact zone, respectively. The above three solutions of differential heat conduction equations obtained under boundary conditions of the second kind and were converted to a uniform dimensionless form, in which the dimensionless temperature depends on the coordinate and dimensionless time multiplicity of the Peclet number, which characterizes this time, the dimensionless half and velocity of the moving heat source. A comparative analysis of surface and deep temperatures was performed for the above three solutions depending on the Peclet number. The possibility of determining the grinding temperature on modern high-speed CNC machines with a one-dimensional solution with $H > 4$ on the basis of computer subsystems of designing, monitoring and diagnosing of grinding operations is shown.

Keywords: Grinding Temperature; Thermal Models; Dimensionless Temperature; Moving Heat Source; Temperature Distribution; Heat Source Shape; Peclet Number

***For citation*: Natalia V. Lishchenko, Vasily P. Larshin. Temperature Models for Grinding System State Monitoring. *Applied Aspects of Information Technology*. 2019; Vol.2 No.3: 216–229. DOI: https://doi.org/10.15276/aait.03.2019.4**

INTRODUCTION

Grinding temperature mathematic models need for the designing, monitoring and diagnosing the grinding operation to boost the operation throughput. This is fully relevant, for example, for CNC gear grinding machines. Once this problem is solved, it becomes possible to develop appropriate computer subsystems to optimize and control the grinding operation on CNC machines at the stages of production and its preparation. The urgency of solving this problem is confirmed by the large number of relevant publications.

The temperature in the grinding zone is one of the main factors limiting the performance of grinding [1, 2], [3]. To optimize a grinding process and boost its productivity, it is necessary to have true information about the grinding temperature which can be obtained by the methods observed in the literature. There are many works which are devoted to the study of thermal phenomena in grinding. In terms of applied research methods the analyzed literary references can be divided into the following groups: theoretical methods [4, 5], [6, 7]; the theoretical ones with experimental verification [8, 9],[10]; theoretical ones with computer simulation of the temperature field [11, 12], [13] computer simulation ones with experimental testing [13, 14], [15, 16], [17, 18]; the only computer simulation ones [19, 20], [21].

The review shows that there is no information about the current grinding temperature in the existing computer systems for monitoring and process diagnostics on CNC grinding machines. This is due to the difficulty of measuring this parameter directly or indirectly.

The state of the problem in the field of the grinding thermophysical theory can be considered taking into account the following philosophical technical concepts that predetermine the corresponding particular approaches to the solution of the corresponding problems. Firstly, it is the concept of dry and wet grinding, which predetermines the absence or accounting of convective heat transfer under the action of grinding fluid. Secondly, it is the concept of macro- and micro-grinding, which allows considering integral (due to averaging) or local heat fluxes

ISSN 2617-4316 (Print)
ISSN 2663-7723 (Online)

with and without taking into account the effect on temperature of instantaneous cutting elements – sections of abrasive grains separated by pores of the grinding wheel (highly porous grinding wheels) as well as their accidental impact on the surface being ground. This concept involves the separation of the grinding process into categories of continuous and discontinuous (with pulsed heat flux), including the grinding with and without convective heat transfer. Thirdly, the concept of super-micro-grinding, which involves taking into account the effect of individual cutting grains of the grinding wheel, with and without taking into account convective heat transfer. The first concept most closely corresponds to the theory of the Jaeger moving heat source [22; 23], on the basis of which simplified formulas for determining the maximum grinding temperature are given in a number of sources without corresponding justifications [4; 6], [24; 25],[26].

In this connection the objective of the study is to develop a simpler temperature model which is acceptable for the modern CNC grinding machines with large values of the workpiece velocity relative to the grinding wheel. In turn, the following tasks rises about the temperature solutions classification, their converting into unique dimensionless form and finding the conditions to simplify the solutions.

CLASSIFICATION, SELECTION AND ANALYSIS OF GRINDING TEMPERATURE MODELS

The grinding temperature determination on the basis of moving strip source mathematical model with the restriction of the source along the Y axis (Fig. 1a) is a complex task of mathematical thermophysics. The task solution is obtained by H.S. Carslaw and J.C. Jaeger [22] for an abstract infinite solid with moving heat strip source on it when the initial temperature of the solid is equal to zero and at a constant of the heat flux density q in the contact zone surface. This solution [22] in our notation has the form

$$T_{2D}(Z,X,H)=\frac{qa}{\pi\lambda V}\times \times\int_{Z-H}^{Z+H}\exp(u)K_0\left(\sqrt{X^2+u^2}\right)du, \quad (1)$$

where: a and λ are the thermal diffusivity in m^2/s and thermal conductivity in W/(m·K) of the workpiece material; V is the heat source velocity, m/s; X, Z are dimensionless (relative) coordinates which correspond to dimensional coordinates x, z in m; H is the dimensionless heat source half-width which correspond to the dimensional half-width h in m; $K_0(s)$ stands for the zeroth-order modified Bessel function of the second kind.

In equation (1) the following designations are used:

$$X=\frac{Vx}{2a};\ Z=\frac{Vz}{2a};\ H=\frac{Vh}{2a}.$$

It is noted in [22] that for large values of H the maximum temperature occurs near $Z=H$ and is approximately $qh/\lambda\sqrt{\pi H}$ which is the value found for the one-dimensional solution at the end of time $2h/V$ for heat supply at the rate of q over a plane in the infinite solid.

The temperature in a semi-infinitive solid (Fig. 1a) is just twice the value (1), i.e.

$$T_{2D}(Z,X,H)=\frac{2qa}{\pi\lambda V}\times \times\int_{Z-H}^{Z+H}\exp(u)K_0\left(\sqrt{X^2+u^2}\right)du. \quad (2)$$

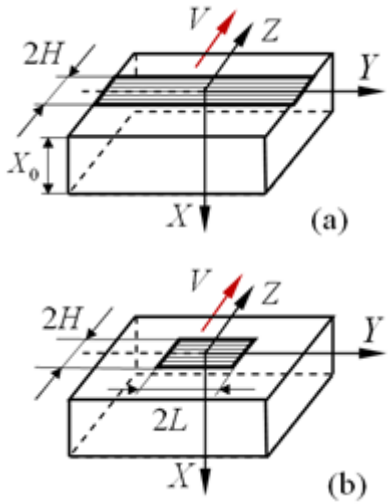

Fig. 1. **Strip (a) and rectangular (b) moving heat sources in a semi-infinitive solid with a sufficiently large size** X_0

***Source*: compiled by the author**

Another problem is the study of the close agreement of three- and two-dimensional solutions of differential equations of heat conduction obtained in [22] under the same second-kind boundary conditions that most closely correspond to the dry grinding process.

The determination of temperature on the basis of the moving strip source mathematical model with the restriction of this source along the Y axis (Fig.1b) is a complex task of mathematical thermophysics. The solution of this problem for the temperature determination at a uniform heat flux q and for the same initial and boundary conditions has the following form [22; 23].

$$T_{3D}(X,Y,Z,L,H) = \frac{2qa}{4\lambda V\sqrt{2\pi}} \times$$
$$\times \int_0^{\infty} \exp\left(\frac{-X^2}{2u}\right)\left(\operatorname{erf}\left(\frac{Y+L}{\sqrt{2u}}\right) - \operatorname{erf}\left(\frac{Y-L}{\sqrt{2u}}\right)\right) \times \quad (3)$$
$$\times \left(\left(\operatorname{erf}\left(\frac{Z+H+u}{\sqrt{2u}}\right) - \operatorname{erf}\left(\frac{Z-H+u}{\sqrt{2u}}\right)\right)\right)\frac{1}{\sqrt{u}}du,$$

where: Y is dimensionless (relative) coordinate which correspond to dimensional coordinate y; L is the dimensionless heat source half-length, which correspond to the same dimensional parameter l in m.

Here it is assumed that: $\xi = \frac{V(z-z')}{2a}$, $L = \frac{Vl}{2a}$, $-h < z < h$, $-l < y < l$. In formula (3) $\operatorname{erf}(s) = \frac{2}{\sqrt{\pi}}\int_0^s \exp\left(-\xi^2\right)d\xi$ is the well-known Gauss error special function.

TRANSFORMING THE TWO-AND ONE-DIMENSIONAL SOLUTIONS

To bring the equation (2) into the coordinate system of the equation (3) it is necessary to change the integration variable $u = -\xi$ in the equation (2) and replace the sign both in integration limits and in variable Z. As a result it is obtained the equation as in works [4], [23], [26; 27], i.e. in the form

$$T_{2D}(Z,X,H) = \frac{2qa}{\pi\lambda V} \times$$
$$\times \int_{Z-H}^{Z+H} \exp(-\xi) K_0\left(\sqrt{X^2+\xi^2}\right)d\xi. \quad (4)$$

For the one-dimensional solution the temperature in the semi-infinitive solid at any point of x at the time τ for unlimited (Fig. 2a) and limited end face area (Fig. 2b) has the form [22]

$$T_{1D}(x,\tau) = \frac{2q\sqrt{a\tau}}{\lambda}\operatorname{ierfc}\left(\frac{x}{2\sqrt{a\tau}}\right). \quad (5)$$

where: $\operatorname{ierfc} u = \frac{1}{\sqrt{\pi}}\exp\left(-u^2\right) - u\cdot\operatorname{erfc} u$.

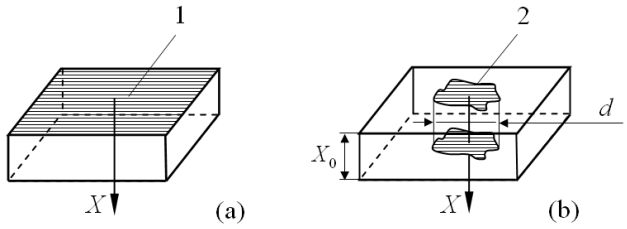

Fig. 2. **Unmoving flat heat source acting fixed time $\tau = 2h/V$ onto a semi-infinite solid withunlimited (a) and limited (b) end faces 1 and 2, respectively (the second kind boundary conditions occur in shaded areas)**
***Source*: compiled by the author**

The surface temperature, i.e. at $x = 0$, is given by [22]

$$T_{1D}^{\max} = \frac{2q}{\lambda}\sqrt{\frac{a\tau}{\pi}}. \quad (6)$$

The grinding temperature from the impact of a short in time heat flux pulse having the duration τ_H (heating time) is described by two equations. The first equation of the two is for the heating time interval of $0 \le \tau \le \tau_H$, and the second is for another time interval of $\tau_H \le \tau < \infty$, i.e. after the heating time is over [22]. Thus,

$$\begin{cases} T_{1D}(x,\tau) = \dfrac{2q\sqrt{a\tau}}{\lambda}\operatorname{ierfc}\left(\dfrac{x}{2\sqrt{a\tau}}\right), \text{if} \quad 0 \le \tau \le \tau_H; \\ T_{1D}(x,\tau) = \dfrac{2q\sqrt{a\tau}}{\lambda}\left\{\sqrt{\tau}\operatorname{ierfc}\left(\dfrac{x}{2\sqrt{a\tau}}\right) - \sqrt{\tau-\tau_H}\operatorname{ierfc}\left(\dfrac{x}{2\sqrt{a(\tau-\tau_H)}}\right)\right\}, \text{if} \quad \tau_H \le \tau < \infty. \end{cases} \quad (7)$$

The time τ in the first equation of the system (7) is ended at $\tau = \tau_H$. During this time, a heat source is moving relative to a fixed point P of the surface (Fig. 3a). Determination of the temperature in the next time interval $\tau_H \le \tau < \infty$ must be made according to the second equation of the system (7). This can be explained by superposition of two solutions of the same type, one of which (the second) has a time offset τ_H relative to the first solution (Fig. 3b).

ISSN 2617-4316 (Print)
ISSN 2663-7723 (Online)

Using the designations adopted above i.e. at $X = \frac{Vx}{2a}$, $H = \frac{Vh}{2a}$, $\tau = \frac{4aB}{V^2}$, and $\tau_H = \frac{4aH}{V^2}$ because of $\tau = 2b / V$, $0 \le 2b \le 2h$ (Fig. 1a) and $\tau = 2h / V$, the equation (5) takes the form

$$T_{1D}(X,B) = \frac{4aq}{\lambda V}\sqrt{B}\,\mathrm{ierfc}\left(\frac{X}{2\sqrt{B}}\right). \qquad (8)$$

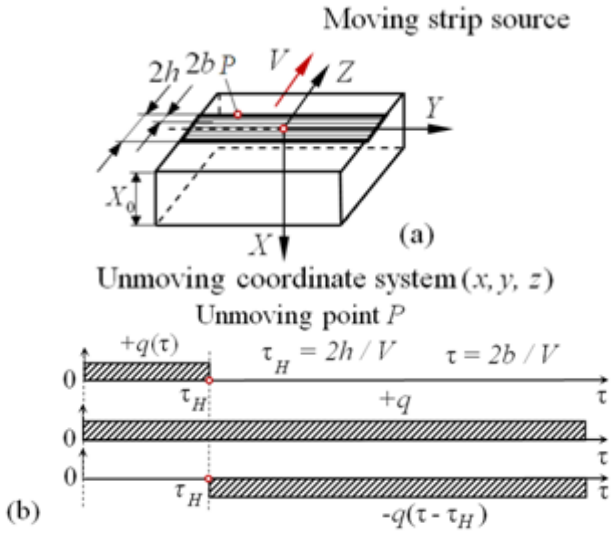

Fig. 3. **Moving strip source in the (x,y,z) unmoving coordinate system referenced to the solid (a) and replacing the heat flux pulse $+q(\tau)$ by superposition of two single-type solutions with heat flux $+q$ and $-q(\tau - \tau_H)$ (b)**

***Source*: compiled by the author**

Thus, at $2b = 2h$ we get $B = H$, i.e. the current value B at fixed value H in the intervals $B \le H$ and $B \ge H$ are the dimensionless time in the one-dimensional solution (8). For the current time $\tau = 2h / V$ from the (5) as well as from the (8) we have the one-dimensional solution maximum temperature according to the equation (6).

Therefore, we conclude that in [22] the following mathematical idea was proposed

$$\lim_{H\to\infty} T_{2D}\Big|_{X=0} = T^{\max}_{2D}\Big|_{X=0} = T^{\max}_{1D}\Big|_{X=0} = \frac{2q}{\lambda}\sqrt{\frac{a\tau}{\pi}}. \qquad (9)$$

If this is so, then a scientific hypothesis arises about the close agreement of the calculation results of the two- and one-dimensional solutions (2) and (8), if the latter will be transforming to the system (7). In addition, a similar results close agreement problem must be considered for the three- and two-dimensional solutions (3) and (4).

PUTTING THE SOLUTIONS IN ONE CO-ORDINATE SYSTEM

Dividing both parts of equations (3), (4) and (8) by the factor of $2qa / \pi\lambda V$, we obtain the following three-,two- and one-dimensional solutions in a dimensionless form, respectively, in the intervals of $-20H \le Z \le +5H$ for the equations (3), (4) and of $-20H \le B \le +5H$ for the equation (8).

Three-dimensional solution in the space interval of $-20H \le Z \le +5H$:

$$\Theta_{3D}(X,Y,Z,L,H) = \sqrt{\frac{\pi}{32}}\int_0^{\infty}\exp\left(\frac{-X^2}{2u}\right)\left[\mathrm{erf}\left(\frac{Y+L}{\sqrt{2u}}\right) - \mathrm{erf}\left(\frac{Y-L}{\sqrt{2u}}\right)\right]\times$$
$$\times\left[\mathrm{erf}\left(\frac{Z+H+u}{\sqrt{2u}}\right) - \mathrm{erf}\left(\frac{Z-H+u}{\sqrt{2u}}\right)\right]\frac{1}{\sqrt{u}}\,du. \qquad (10)$$

Two-dimensional solution in the space interval of $-20H \le Z \le +5H$:

$$\Theta_{2D} = \Theta(X,Z,H) = \int_{Z-H}^{Z+H}\exp(-\xi)\,K_0\left(\sqrt{X^2+\xi^2}\right)d\xi. \qquad (11)$$

One-dimensional solution in the time interval of $B \le H$ [28, 29]:

$$\Theta_{1D} = \Theta(X,B) = 2\pi\sqrt{B}\,\mathrm{ierfc}\left(\frac{X}{2\sqrt{B}}\right). \qquad (12)$$

Now for the equations (10), (11) and (12) the intervals of change in the dimensionless spatial coordinate Z, which measured in units of the dimensionless half-width of the moving heat source (the Peclet number) for equations (3) and (4),coincide with the corresponding intervals of change in the dimensionless time coordinate B for the equation (8).

By analogy with equation (7) the dimensionless grinding temperature from the impact of a short pulse of heat flux having duration τ_H is described by the two interconnected equations. The first equation of the two is for the time interval of heating $0 \le B \le H$, and the second is for another time interval $H \le B \le \infty$ (e.g. $-20H \le B \le +5H$), i.e.

$$\begin{cases} \Theta_{1D} = \Theta(X,H) = 2\pi\sqrt{B}\ \text{ierfc}\dfrac{X}{2\sqrt{B}}, \text{if} \quad 0 \le B \le H; \\ \Theta_{1D} = \Theta(X,H) = 2\pi\left(\sqrt{B}\ \text{ierfc}\dfrac{X}{2\sqrt{B}} - \sqrt{B-H}\ \text{ierfc}\dfrac{X}{2\sqrt{B-H}}\right), \text{if} \quad H \le B < \infty. \end{cases} \tag{13}$$

Moreover, the fixed value H in equations (10) and (11) corresponds to the fixed value $H = \dfrac{V^2}{4a}\tau_H$ in equation (13). That is, the $H = \dfrac{V^2}{4a}\tau_H$ in equation (13) is the dimensionless half-width of the heat source, which characterizes the interval of the dimensionless time of the heat source action at the heating stage.

To ensure the comparability of solutions (10), (11) and (13) along the abscissa axis, they must be converted to represent in the same coordinate system, which is moving for the equations (10) and (11) (MCS in Fig. 4) with speed V, while for the equation (13) this coordinate system is unmoving (UCS in Fig. 4).

To do this, it is necessary to fulfill two conditions. Firstly, that the starting and ending points of the heating correspond to the spatial coordinates $Z = +H$ and $Z = -H$ for the three- and two-dimensional solutions (10) and (11). Secondly, the distance along the coordinate Z between these points in the moving coordinate system, i.e. the distance $\Delta Z = 2H$, corresponded to the dimensionless heating time H (it corresponds to the dimensional time of $\tau_H = 2h/V$) in the unmoving coordinate system. For this, the equation (13) must be subjected to the following three transformations: (1) introduce a new variable $H' = H/2$ (or $2H' = H$) along the abscissa axis; (2) position the region of variation of the argument along the abscissa axis on its negative semi-axis (Fig. 4b); (3) shift the abscissa of the entire dependence by the value $H' = H/2$ to the left (in Fig. 4 it is not shown) so that the zero coordinate on the abscissa axis for the equations (10); (11) and (13) coincides with the zero coordinate on the abscissa axis for the equation (13).

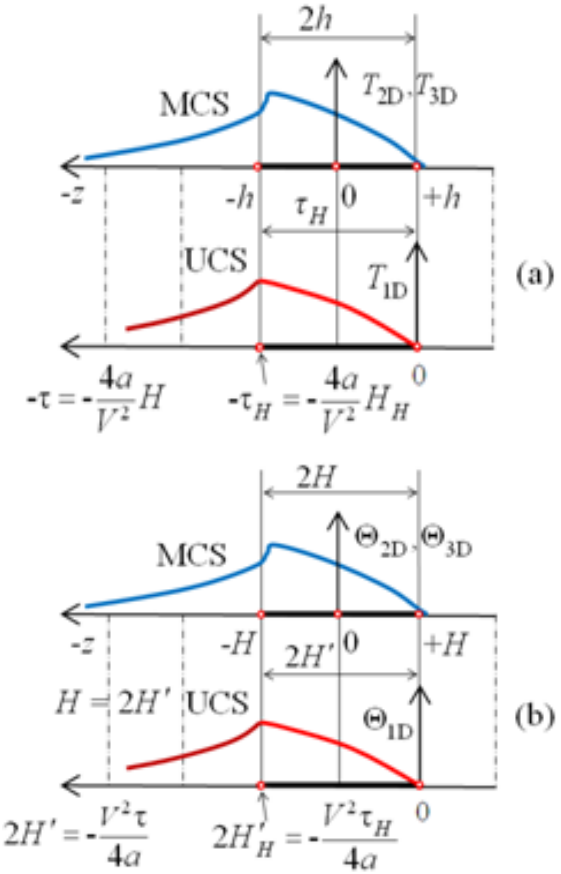

Fig. 4. **Ensuring comparability of moving (MCS) and unmoving (UCS) coordinate systems for determining grinding temperature using dimensional (a) and dimensionless (b) parameters**
***Source*: compiled by the author**

After these three transformations, equation (13) takes the following form:

ISSN 2617-4316 (Print)
ISSN 2663-7723 (Online)

$$\begin{cases} \Theta'_{1D} = \Theta'(X,B,H) = 2\pi\sqrt{|0.5(B-H)|}\ \text{ierfc}\dfrac{X}{2\sqrt{|0.5(B-H)|}}, & \text{if } -H \le B \le 0;\ \square \\ \Theta'_{1D} = \Theta'(X,B,H) = 2\pi\sqrt{|0.5(B-H)|}\ \text{ierfc}\dfrac{X}{2\sqrt{|0.5(B-H)|}} - & \\ \quad -2\pi\sqrt{H_H(0.5(B-H)-1)}\ \text{ierfc}\dfrac{X}{2\sqrt{H(0.5(B-H)-1)}}, & \text{if } -20H \le B \le -H. \end{cases} \quad (14)$$

Now in equations (10), (11) and (14), the parameter H is the dimensionless Peclet number [4, 7]. Moreover, in equations (10) and (11) the parameter H characterizes the dimensionless spatial coordinate Z while in equation (14) – the time dimensionless coordinate B.

Next, in equations (10) and (11) we introduce a variable $f = Z / H$, and in equation (14) – a variable $f = B / H$.

This provides the same presentation format of these three equations, in which the abscissa axis for equations (10), (11) and (14) is represented in the values of the same variable f which is multiple to the Peclet number H.In this case, equations (10), (11) and (14) take the following form.

Three-dimensional solution in the space interval of $-20 \le f \le +5$, where $f = Z / H$:

$$\Theta_{3D}(X,Y,L,H,f) = H\sqrt{\frac{\pi}{32}} \times \int_0^{\infty/H} \exp\left(\frac{-X^2}{2Hf}\right)\left\{\text{erf}\left(\frac{Y+L}{\sqrt{2Hf}}\right) - \text{erf}\left(\frac{Y-L}{\sqrt{2Hf}}\right)\right\} \times$$
$$\times\left[\text{erf}\left(\frac{Z+H+Hf}{\sqrt{2Hf}}\right) - \text{erf}\left(\frac{Z-H+Hf}{\sqrt{2Hf}}\right)\right]\frac{1}{\sqrt{Hf}}\,df. \quad (15)$$

Two-dimensional solution in the space interval of $-20 \le f \le +5$, where $f = Z / H$:

$$\Theta_{2D} = \Theta(X,H,f) = H\int_{f-1}^{f+1} \exp(-\alpha H)\,K_0\left(\sqrt{X^2 + (\alpha H)^2}\right)d\alpha. \quad (16)$$

where: α is a new integration variable.

One-dimensional solution in the time intervals of $-1 \le f \le +1$ and $-20 \le f \le -1$ where $f = H / H_H$:

$$\begin{cases} \Theta'_{1D} = \Theta'(X,H,f) = 2\pi\sqrt{0.5H|f-1|}\ \text{ierfc}\dfrac{X}{2\sqrt{0.5H|f-1|}}, & \text{if } -1 \le f \le +1; \\ \Theta''_{1D} = \Theta''(X,H,f) = 2\pi\sqrt{0.5H|f-1|}\ \text{ierfc}\dfrac{X}{2\sqrt{0.5H|f-1|}} - & \\ \quad -2\pi\sqrt{H(0.5|f-1|-1)}\ \text{ierfc}\dfrac{X}{2\sqrt{H(0.5|f-1|-1)}}, & \text{if } -20 \le f \le -1. \end{cases} \quad (17)$$

EXPLORING THE DIFFERENCE BETWEEN THREE- AND TWO-DIMENSIONAL SOLUTIONS

To explore a grinding scheme let's change the source velocity at a fixed half-width of the source $2H$. For example, for profile gear grinding scheme with $h = 2.72 \cdot 10^{-3}$ m ($h = \sqrt{Dt_v} / 2$; $t_v = 0.074 \cdot 10^{-3}$ m; D =0.4 m) at the rear edge $Z = -H$ on the surface X =0, $y / l = 0\ldots1/5$, and a =5.683·10^{-6}м^2/s it is selected three forms of contact spots: the rectangular elongated along the axis $0Y$; the square; the rectangular elongated along the axis $0Z$. To provide

these forms, the length l of the source was chosen as follows: $l = 11 \cdot 10^{-3}$m ($H / L = 0.2474$; Fig. 5a); $l = 3{,}469 \cdot 10^{-3}$m ($H / L = 0.7847$; Fig. 5b); $l = 1 \cdot 10^{-3}$m ($H / L = 2.7235$; Fig. 5c).

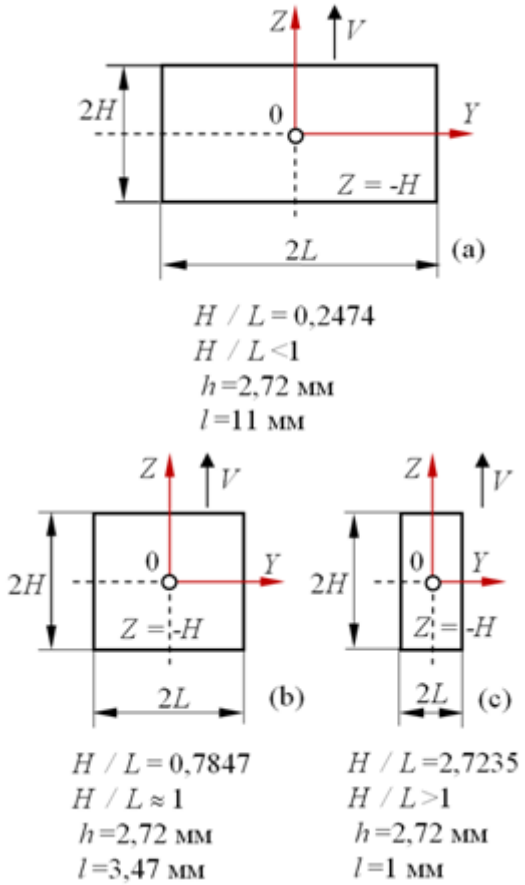

Fig. 5. **Three configurations of rectangular sources for research**

***Source*: compiled by the author**

The choice of these three H / L relations obtained by changing l at h = const =2.72 mm is due to the need for a characteristic change in the shape of a rectangular source, namely: H / L =0.2474 <1 (Fig. 5a); H / L = 0.7847≈1 (Fig. 5b) and H / L = 2.7235>1 (Fig. 5, c). Dimensionless parameters H and L is changed due to discrete change in the velocity of the source in the range of grinding modes: V = 0.2 m/min (0.0033 m/s), V =0.5 m/min (0.0083 m/s); V = 1 m/min (0.017 m/s); V = 2 m/min (0.033 m/s); V = 4 m/min (0.067 m/s); V = 5 m/min (0.083 m/s); V = 7 m/min (0.117 m/s); V = 10 m/min (0.167 m/s); V = 12 m/min (0.2 m/s).

As an example, it is calculated the profile gear grinding temperature on the surface by the equation (10) multiplied by the $\frac{2qa}{\pi\lambda V}$ with the following initial data: q =22,7·10^6 W/m^2; a =5.683·10^{-6} m^2/s; λ =24 W/(m·°C); V =0.2 m/s (12 m/min); z =0; h =2.72·10^{-2} m (D =0.4 m; t_v =0.074·10^{-3} m); l =3.469·10^{-3} m; $-5H \le Z \le 5H$; X =0 (on the surface); H =47,869; L =61. The coordinates along the y axis are the following: y = 0, i.e. Y =0; $y = l / 2$, i.e. Y =8.799; $y = 3l / 4$, i.e. Y =13.198; $y = 7l / 8$, i.e. Y =15.397; $y = l$, i.e. Y =17.597. The maximum temperatures are located about at the back edge of the moving heat source, i.g. at $Z = -0{,}95H$ (Fig. 6).

An idea of the result close agreement of three-, two-, and one-dimensional solutions is to determine the conditions under which the calculation by any of these equations yields very close results, e.g. with the difference which is less than 5 %. That is why, under these conditions it becomes possible to use the simpler one-dimensional solution instead of three- and two-dimensional ones. In order to show the congruent continuity of equations (10) and (11), it is performed the study of the temperature field along the heat source length in the direction of the $0Y$ axis by the equation (10). To make the study more general, it is executed in dimensionless form using equations (10) and (11). To fit the actual grinding scheme let the half-width of the source h will be equal to 2.72·10^{-3} m and the temperature will be considered at the back edge of the heat source, i.e. at $Z = -H$. Besides, let $X = 0$ when the temperature is determined on the workpiece surface at the interval of $0 \le y / l \le 1.5$, and at a = 5,683·10^{-6} m^2/s. It is selected three contact spot shapes: a rectangular shape which is elongated along the $0Y$ axis; a square shape which is equally elongated along both $0Y$ and $0Z$ axes; a rectangular shape which is elongated along the $0Z$ axis. To provide these three shapes, the length of the moving heat source was chosen as follows: l =11·10^{-3} m (H / L = 0.2474); l =3.469·10^{-3} m (H / L = 0,7847); l = 1·10^{-3} m (H / L = 2,7235).

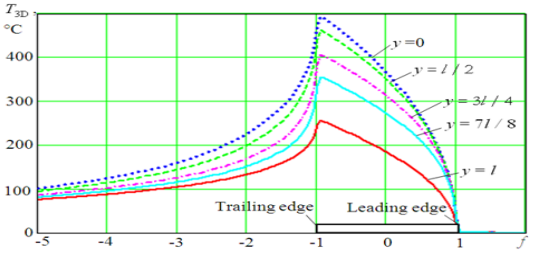

Fig. 6. **Surface temperature vs the $Z / H = f$ dimensionless coordinate which coincides with the moving heat source velocity vector (at different values of y)**

***Source*: compiled by the author**

The choice of these three H / L relations which are obtained by changing the l at the same h

ISSN 2617-4316 (Print)
ISSN 2663-7723 (Online)

=2.72 mm is due to the need for a characteristic change in the shape of a rectangular source: H / L <1; H / L =1, and H / L > 1. Dimensionless parameters H and L are changed due to discrete change in the velocity of the moving heat source in the range of the following grinding modes: V = 0.2 m/min (0.0033 m/s), V = 0.5 m/min (0.0083 m/s); V =1 m/min (0.017 m/s); V = 2 m/min (0.033 m/s); V = 4 m/min (0.067 m/s); V = 5 m/min (0.083 m/s); V = 7 m/min (0.117 m/s); V = 10 m/min (0.167 m/s); V =12 m/min (0.2 m/s). Then the dimensionless temperatures were calculated by the equation (10) and (11) for the three indicated characteristic configurations of the moving rectangular heat source: H / L <1 (Fig. 7a), $H / L \approx 1$ (Fig. 7b) and H / L > 1 (Fig. 7c) on the heat source back edge, that is at Z = -H for the interval of $0 \le Y / L \le 1.5$.

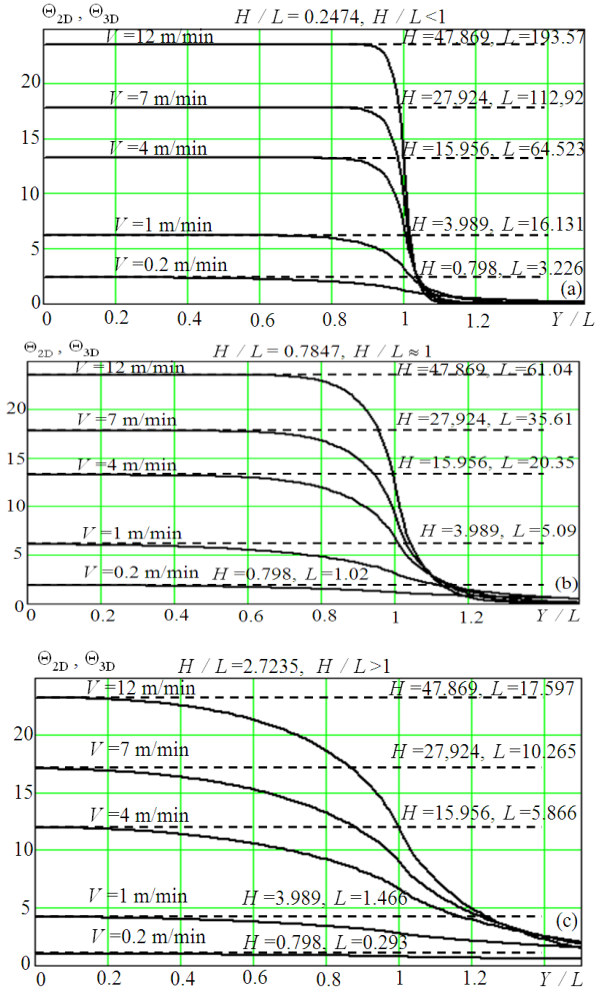

Fig. 7. **The temperatures Θ_{3D} (straight horizontal lines) and Θ_{2D} (curved dotted lines) vs ratio of Y / L for the moving heat source rectangular shape which is elongated along the $0Y$ axis at H / L = 0.2474, i.e. at H / L <1 (a), $H / L \approx$ 1 (b) and H / L > 1 (c)**

***Source*: compiled by the author**

Figure 7 shows that the difference between the maximum temperatures Θ_{3D} and Θ_{2D} which is observed only in a certain zone located in the vicinity of point at Y = L. At Y =0 and at heat source back edge (Z = -H) there is practically no difference between temperatures Θ_{3D} and Θ_{2D}. But for the H / L =1 and H / L >1 the difference increases. For example, the results of calculating the dimensionless temperature by equations (10) and (11) for l = $3.469 \cdot 10^{-3}$ m and H / L =0,7847 (it is close to square shape), Z = -H, and Y =0 are summarized in Table 1.

Table 1. **Dimensionless temperatures for the rectangular and strip moving sources**

V, m/min	0,2	1,0	5,0	7,0	12,0
H	0,798	3,989	19,946	27,924	47,87
L	1,017	5,087	25,435	35,609	61,04
Θ_{3D}	**1,869**	6,066	**14,879**	17,772	23,56

***Source*: compiled by the author**

Table 1 shows that as the velocity of the rectangular and strip sources increases the difference in the surface temperatures Θ_{3D} and Θ_{2D} on the heat sources back edges (Z = -H) at Y = 0 decreases. The temperatures calculated by equations (10) and (11) practically are close agreement at V >5 m/min. To determine the divergence between the calculation results by equations (10) and (11), i.e. on the back edge of the moving heat source (Z = -H) and at Y =0 (center of the heat source) when X =0 (surface), it is determined the ratio of the dimensionless temperature by the equation (10) for the rectangular source to the temperature by the equation (11) for the strip source, that is it is defined the coefficient or degree of the temperature decrease $k = \Theta_{3D} / \Theta_{2D}$.

This study shows that when H / L <1, on the one hand, and as the Peclet number grows, on the other hand, the difference in the results of calculating the maximum temperatures for the three- and two-dimensional solutions decreases.

EXPLORING THE DIFFERENCE BETWEEN TWO- AND ONE-DIMENSIONAL SOLUTIONS

The results of the temperature field calculation by equations (16) and (17) are presented in Fig. 8, respectively in the left (Fig. 8a) and right (Fig. 8b).

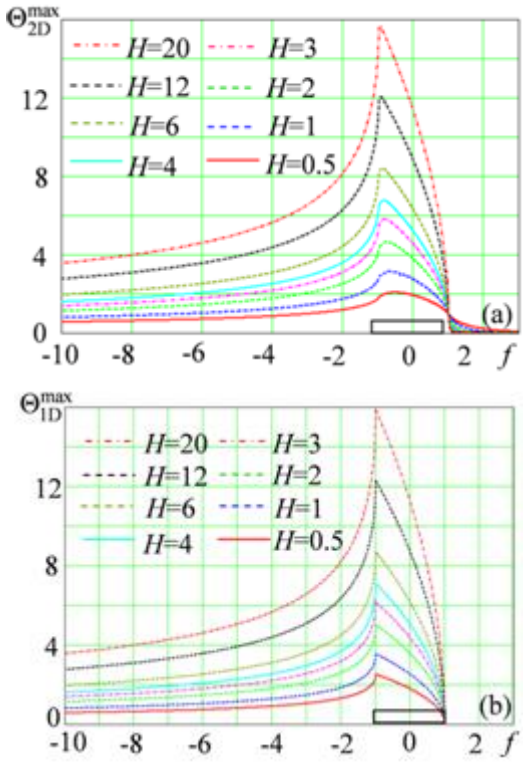

Fig. 8. **Surface (X =0) temperature distribution for the two- (a) and one-dimensional (b) solutions**

***Source*: compiled by the author**

The maximum temperature found by the two-dimensional solution (24) is shifted to the trailing edge of the source with the coordinate of $f = Z / H = -1$, but does not coincide with it. The position of the maximum temperature varies depending on H (Fig. 9a). At H =20, the maximum temperature is practically at the trailing edge of the source (Fig. 8a). For example, at H =0.5 we have Z / H =-0,536, at H =5, Z / H = -0,876, at H = 20, Z / H = -0.955. At the same time, the maximum temperature found from the one-dimensional solution (25) always takes place at f = -1 (heating time end in the one-dimensional solution) for all values of H (Fig. 8b).

So, the solutions (16) and (17) allow calculating the temperature field during grinding. For the purpose of demarcation of the solution (17) with a ceiling not exceeding 5 % compared to the solution (16), the maximum temperature is calculated by the solutions with the aid of MathCAD medium in the intervals of $0{,}5 \le H \le 20$ and $0 \le X \le 3$. The difference between the calculation results by the solutions (24) and (25) as a function of H is shown in Fig. 9b.

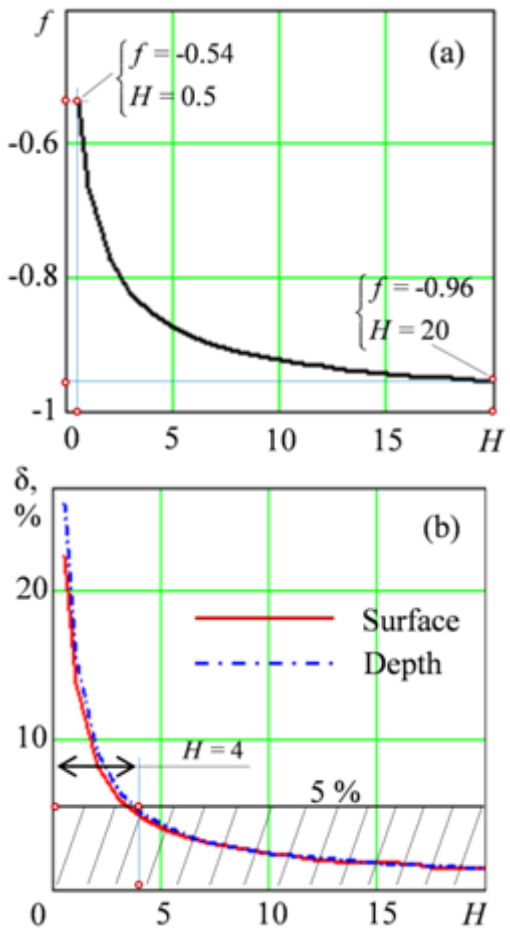

Fig. 9. **Position of the temperature peak on the surface according to the two-dimensional solution (16) depending on H (a) and the difference (in percent) between the results of determining the maximum temperatures by solutions (16) and (17) on the surface (Surface) and at the depth (Depth) of the double temperature drop (b)**

***Source*: compiled by the author**

The red line ("Surface" in Fig. 9b) is the difference of the maximum surface temperatures found by equations (16) and (17), and the blue line ("Depth" in Fig. 9b) is the difference of temperatures by solutions (16) and (17) at the depth of the double temperature drop found according to equation (16). There is one feature that should be noted as for maximum deep temperature by the solution (17). It lies in the fact that the counting of the deep temperature according to the solution (17) is taken in the coordinate f = -1 (Fig. 10b), which gives a slightly lower temperature than the maximum possible for this solution. As result in the shaded zone (Fig. 9b) the difference between the solutions (16) and (17) does not exceed 5 %. It means that at $4 \le H \le 20$ the solution (17) with sufficient accuracy for practice can be used to calculate the maximum surface and deep temperatures.

ISSN 2617-4316 (Print)
ISSN 2663-7723 (Online)

The temperature field obtained from the two-dimensional solution (16) begins to form ahead of the source at $f > +1$ in the entire range of $4 \le H \le 20$ (Fig. 8a). The temperature field obtained from the one-dimensional solution (Fig. 8b) begins to form at $f = +1$, which corresponds to the start heating time point $\tau = 0$. But with the Peclet number more than 4 (fast moving heat source at $H \ge 4$), the temperature field is formed almost at the leading edge of the source, i.e. at $f = +1$.

The formation of the temperature field obtained by the two-dimensional solution (16) with small Peclet numbers ($H \le 4$) is shown in Fig. 10a.

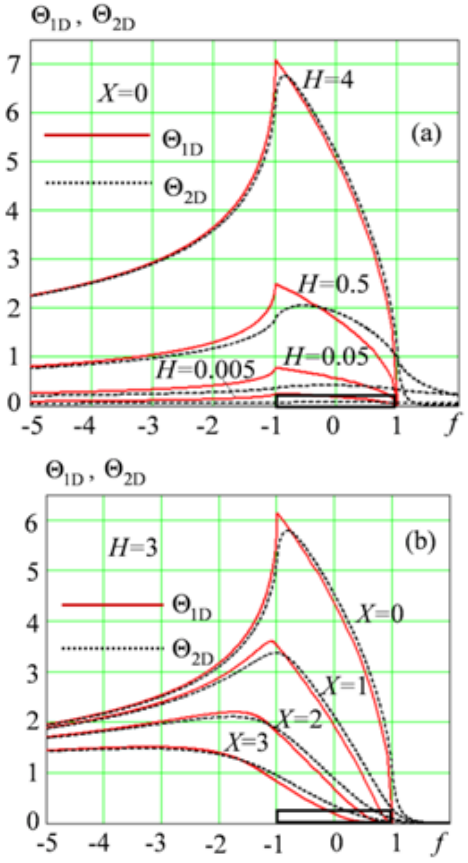

Fig. 10. **Maximum surface (X =0) temperature distribution for the two- and one-dimensional solutions (a) and temperature distributions at various depths below the surface at H =3 (b)**

***Source*: compiled by the author**

Fig. 10a shows that as the Peclet number H decreases, the temperature field according to the two-dimensional solution (16) is more and more ahead of the moving heat source, while for the one-dimensional solution (17) the temperature field, regardless of H, always starts at the point of $f = +1$ in which a heat source starts.

Under otherwise equal conditions, the maximum temperatures found from the two-dimensional solution (16) are always lower than the maximum temperatures found from the one-dimensional solution (17) for both surface and deep temperatures both at different values H (Fig. 10, a) and at various values of X (Fig. 10, b), but this difference decreases with increasing of H.

The maximum temperatures even at H =1 found from the two- and one-dimensional solutions (16) and (17) are close (Fig. 11, a) while at H = 10 they are almost coincide (Fig. 11, b).

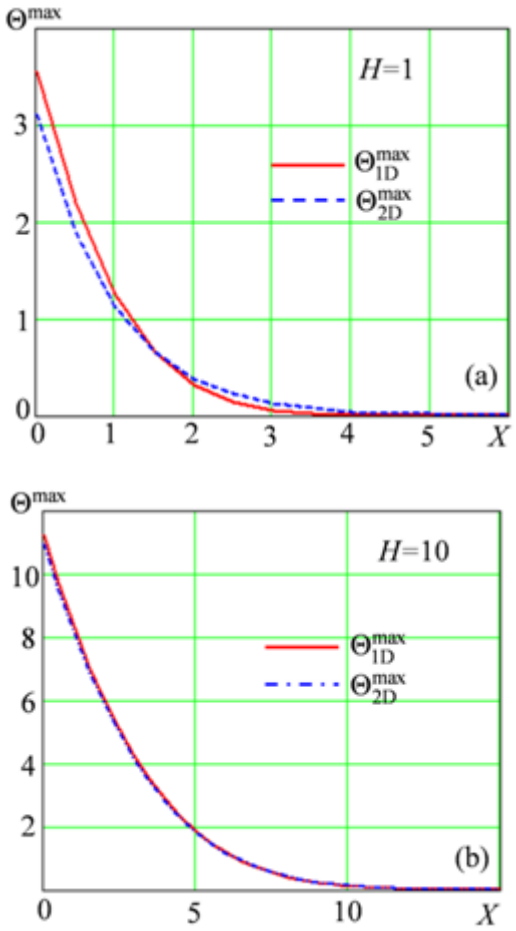

Fig.11. **Maximum temperature vs depths below the surface for Peclet number of H =1 (a) and H =10 (b)**

***Source*: compiled by the author**

In Fig. 11 the maximum temperature Θ_{1D}^{max}, as it was noted above, is taken at f = -1. That is, the temperature determined in this way does not correspond to its theoretical maximum value which takes place at f <,-1 (Fig. 10b) and depends on the depth X. For example, at X =1 and X =2 we have f = -1,1 and f = -1,5, respectively (Fig. 10b). For this case, the ratio of taken temperature at f = -1 to its maximum value at f = -1,1 and f = -1,5 is about of 0,98 and 0,86 instead of 1. The deviation of this ratio from the unit contributes to the convergence of the results of determining the maximum temperature by the two- and one-dimensional solutions (Fig. 11).

CONCLUSIONS AND PROSPECTS FOR-FURTHER RESEARCH

1. A classification of the three-, two- and one-dimensional solutions of differential equations of heat conduction with the same initial and boundary conditions, which best meet the grinding conditions, was performed.

2. These solutions were converted to a typical dimensionless form, allowing investigating the temperature field at the stages of heating the surface to be ground and its cooling (there is no heating) depending on the dimensionless parameter f, which is equal to the Z / H for three- and two-dimensional solutions, and to the B / H for one-dimensional one. In the first case, the variable f is the ratio of the spatial dimensionless parameters while in the second – of the time dimensionless parameters. Thus, the variable f is a twice dimensionless parameter.

3. For large values of Peclet number ($H \geq 4$) the results close agreement of the two- and one-dimensional solutions of the differential equations of heat conduction has been established, which allows replacing complex analytical solutions with simpler ones that can be used in the grinding subsystems of designing, monitoring and process diagnosing on the CNC grinding machines, e.g. in the profile gear grinding.

4. The analysis of the maximum temperatures obtained from the two- and one-dimensional solutions depending on the Peclet number H magnitude, which characterizes the dimensionless velocity of the moving heat source, was performed. It is shown that if the Peclet number is greater than or equal to 4 ($H \geq 4$), the determination of the temperature both on the surface of the workpiece and at a depth of two-fold temperature drop can be made on the basis of the one-dimensional solution with a difference in determining the maximum temperature, compared to the two-dimensional solution, of no more than 5 %.

5. In general, for the three-, two- and one-dimensional solutions there are two results close agreement conditions. Firstly, for the rectangular shape of the contact spot with the overall dimensions of $2H \times 2L$, it is necessary to check the condition $H / L < 1$. For $H / L = 1$ and $H / L > 1$ the close agreement is violated. Secondly, as it was mentioned above the Peclet number H should be greater than or equal to 4 ($H \geq 4$), which corresponds to a fast moving heat source and multi-strokes speed grinding modes on modern CNC machines, e.g. in the profile gear grinding.

REFERENCES

1. Larshin, V. & Lishchenko, N. “Gear grinding system adapting to higher CNC grinder throughput”. *MATEC Web of Conferences*. 2018; Vol. 226(04033). DOI: https://doi.org/10.1051/matecconf /201822 604033.

2. Larshin, V. & Lishchenko, N. “Adaptive Profile Gear Grinding Boosts Productivity of this Operation on the CNC Machine Tools”. *In:1st International Conference on Design, Simulation and Manufacturing,* DSMIE 2018, Sumy, Ukraine, Lecture Notes in Mechanical Engineering. *Publ. Springer*. Cham. 2019. p. 79–88. DOI: https://doi.org/10.1007/978-3-319-93587-4_9.

3. Larshin, V. & Lishchenko, N. “Research Methodology for Grinding Systems”. *Russian Engineering Research.* 2018; Vol.38 Issue 9: 712–713. DOI: https://doi.org/10.3103/S1068798X1809024.

4. Deivanathan, R. & Vijayaraghavan, L. “The oretical analysis of thermal profile and heat transfer in grinding”. *International Journal of Mechanical and Materials Engineering.* (IJMME). 2013; Vol. 8 Issue 1: 21–31.

5. Anto´nio, T. & Simo˜es, N. “Three-dimensional fundamental solutions for transient heat transfer by conduction in an unbounded medium, half-space, slab and layered media”. *Engineering Analysis with Boundary Elements.* 2006; Vol.30 Issue 5:338–349. DOI: https://doi.org/10.1016/j.enganabound. 2006.01.011.

6. González-Santander, J. L. “Maximum Temperature in Dry Surface Grinding for High Peclet Number and Arbitrary Heat Flux Profile”. *Hindawi Publishing Corporation Mathematical Problems in Engineering.* 2016; Vol.2016: 1–9. Article ID 8470493. DOI: http://dx.doi.org/10.1155/2016/8470493.

7. Guo, C. & Malkin, S. “Analysis of Transient Temperatures in Grinding”. *Journal of Engineering for Industry.* 1995; Vol.117 Issue 4: 571–577. DOI: https://doi.org/10.1115/1.2803535.

8. Tan, J., Jun, Y. & Siwei, P. “Determination of burn thresholds of precision gears in form grinding based on complex thermal modelling and Barkhausen noise measurements”. *The International Journal of Advanced Manufacturing Technology*. 2017; Vol.88, Issue 1-4: 789–800.

ISSN 2617-4316 (Print)
ISSN 2663-7723 (Online)

9. Jun, Y. & Ping, L. “Temperature distributions in form grinding of involute gears”. *The International Journal of Advanced Manufacturing Technology*. 2017; Vol.88 Issue 9-12: 2609–2620. DOI: https://doi.org/10.1007/s00170-016-8971-z.

10. Malkin, S. & Guo, C. “Thermal Analysis of Grinding”. *CIRP Annals Manufacturing Technology.* 2007; Vol.56, Issue 2: 760–782. DOI: https://doi.org/10.1016/j.cirp.2007.10.005.

11. Foeckerer, T., Zaeh, M. & Zhang, O. „A three-dimensional analytical model to predict the thermo-metallurgical effectswithin the surface layer during grinding and grind-hardening. International”. *Journal of Heat and Mass Transfer*. 2013; Vol.56 Issue 1-2: 223–237. DOI: https://doi.org/10.1016/ j.ijheatmasstransfer. 2012.09.029.

12. Mahdi, M. & Liangchi, Z. “The finite element thermal analysis of grinding processes by ADINA”. *Computers & Structures*. 1995; Vol.56 Issue 2-3: 313–320. DOI: https://doi.org/10.1016/0045-7949(95)00024-B.

13. Wang, L., Qin, Y., Liu, Z-c. & Ge, P-q. “Computer simulation of a workpiece temperature field during the grinding process”. Proceedings of the Institution of Mechanical Engineers Part B: *Journal of Engineering Manufacture*. 2003; Vol.217 Issue 7: 953–959. DOI:https://doi.org/10.1243 /09544050360686824.

14. Linke, B., Duscha, M., Vu, A. T. & Klocke, F. “FEM-based simulation of temperature in speed stroke grinding with 3D transient moving heat sources”. *Advanced Materials Research.* 2011; Vol.223: 733–742. DOI: https://doi.org/10.4028/ www.scientific.net/AMR.223.73.

15. Zhang, L. “Numerical Analysis and Experimental Investigation of Energy Partition and Heat Transfer in Grinding”. In: M. SalimNewazKazi (Eds.) *Heat Transfer Phenomena and Applications. Sense Publishers.* Rotterdam: The Netherlands. 2012. p. 79–98. DOI: https://doi.org/10.5772/52999.

16. Biermann, D. & Schneide, M. “Modeling and simulation of workpiece temperature in grinding by finite element analysis”. *Machining Science and Technology: An International Journal*. 1997; Vol. 9, Issue 2: 173–183. DOI: https://doi.org/10.1080/10940349708945645.

17. Brinksmeier, E., Aurich, J. S., Govekar, E., Heinzel, C., Hoffmeister, H.-W., Klocke, F., Peters, J., Rentsch, R., Stephenson, D. J., Uhlmann, E., Weinert, K. & Wittman, M. „Advances in Modeling and Simulation of Grinding Processes, Annals of the CIRP”. 2006; Vol.55, Issue 2: 667–696. DOI: https://doi.org/10.1016 /j.cirp.2006.10.003.

18. AL-Mokhtar, Mohamed, O., Warkentin, A., & Bauer, R. “Variable heat flux in numerical simulation of grinding temperatures”. Int J AdvManufTechnol. 2006; Vol.63, Issue 5-8: 549–554. DOI: https://doi.org/10.1007/s00170-012-3948-z.

19. Tahvilian, A. M., Champliaud, H., Liu, Z. & Hazel, B. “Study of workpiece temperature distribution in the contact zone during robotic grinding process using finite element analysis”. *In: 8th CIRP Conference on Intelligent Computation in Manufacturing Engineering.* Ischia: Italy. 2013. p. 205–210.

20. Sharma, C., Ghosh, S. & Talukdar, P. “Finite element analysis of workpiece temperature during surface grinding of income 718 alloy”. *In: 5th international & 26th all India manufacturing technology, design and research conference, IIT Guwahati.* Assam: India. 2014. p.420-1–420-6.

21. Yadav, Mr. R. K. “Analysis of grinding process by the use of finite element methods”. *ELK Asia Pacific Journal of Manufacturing Science and Engineering*. 2014; Vol.1, Issue 1: 35–42.

22. Carslaw, H. S. & Jaeger, J. S. “Conduction of Heat in Solids”. Oxford University Press; 2 ed. Great Britain: Oxford. 1959.

23. Jaeger, J. C. “Moving Sources of Heat and Temperature at Sliding Contacts”. Proceedings of the Royal Society. New South Wales. 1942; Vol.76: 203–224.

24. Malkin, S. & Guo, C. “Grinding Technology: Theory and Application of Machining with Abrasives”. *Industrial Press.Inc*. New York: 2008.

25. Akbari, M., Sinton, D. & Bahrami, M. „Geometrical Effects on the Temperature Distribution in a Half-Space Due to a Moving Heat Source, J. Heat Transfer”. 2011; Vol.133 Issue 6: 064502-1–064502-10.

26. Sipaylov, V. A. “Teplovye protsessy pri shlifovanii i upravlenie kachestvom poverkh-nosti, [Thermal processes during grinding and surface quality control]” (in Russian). *Publ.Mashinostroenie*. Moscow: Russian Federation. 1978.

27. Lishchenko, N. V. & Larshin, V. P. “Profile Gear Grinding Temperature Determination. In: 4th International Conference on Industrial Engineering”. *ICIE, Lecture Notes in Mechanical Engineering*. *Publ. Springer*. 2019. p. 1723–1730. DOI: https://doi.org/10.1007/978-3-319-95630-5_185.

28. Lavine, A. S. “A Simple Model for Convective Cooling During the Grinding Process”. *Journal of Engineering for Industry.* 1998; Vol.110, Issue 1: 1–6.

29. Larshin, V. P, Kovalchuk, E. N. & Yakimov, A. V. “Primenenie resheniy teplofizicheskikh zadach k raschetu temperatury i glubiny defektnogo sloya pri shlifovanii” (in Russian). [Application of solutions of thermophysical problems to the calculation of the temperature and depth of the defective layer during grinding]. Interuniversity collection of scientific works, Perm. 1986. p. 9–16

Conflicts of Interest: the authors declare no conflict of interest

Received 03.04.2019
Received after revision 07.06.2019
Accepted 18.06.2019

DOI:https://doi.org/10.15276/aait.03.2019.4
УДК 004.942:621.923

ТЕМПЕРАТУРНІ МОДЕЛІ ДЛЯ МОНІТОРИНГУ СТАНУ ТЕХНОЛОГІЧНОЇ СИСТЕМИ ШЛІФУВАННЯ

Наталя Володимирівна Ліщенко[1)]
ORCID: 0000-0002-4110-1321; odeslnv@gmail.com
Василь Петрович Ларшин[2)]
ORCID: 0000-0001-7536-3859; vasilylarshin@gmail.com
[1)] Одеська національна академія харчових технологій, вул. Канатна, 112. Одеса, 65039, Україна
[2)] Одеський національний політехнічний університет, пр. Шевченка, 1. Одеса, 65044, Україна

АНОТАЦІЯ

Температура шліфування обмежує продуктивність цієї операції і є важливим параметром для оцінки стану технологічної системи. Однак в існуючих комп'ютерних системах моніторингу та технологічної діагностики на верстатах з ЧПК інформація про поточну температурі шліфування відсутня. Це викликано труднощами прямого і непрямого вимірювання цього параметра. У першому випадку – труднощами з установкою датчиків температури, у другому – відсутні прийнятні математичні моделі для визначення температури шліфування. Мета дослідження - розробка більш простої температурної моделі, яка буде прийнятною для сучасного шліфування з великими значеннями швидкості заготовки щодо шліфувального круга. Для досягнення мети дослідження була виконана класифікація рішень три-, дво- і одновимірного диференціальних рівнянь теплопровідності з однаковими початковими і граничними умовами для дослідження температур шліфування за допомогою цих рішень при інших рівних умовах. Умови близького узгодження результатів рішень встановлюються в залежності від геометричної конфігурації зони контакту між шліфувальним кругом і заготовкою: $H / L < 1$ і $H > 4$, де H і L - половина ширини і половина довжини зони контакту, відповідно. Вищезазначені три рішення диференціальних рівнянь теплопровідності отримано при граничних умовах другого роду і були перетворені в однорідну безрозмірну форму, в якій безрозмірна температура залежить від координати і кратності безрозмірного часу числу Пекле, яке характеризує цей час, а також безрозмірні півширину і швидкість рухомого джерела тепла. Порівняльний аналіз поверхневих і глибинних температур був виконаний для трьох зазначених вище рішень в залежності від числа Пекле. Показана можливість визначення температури шліфування на сучасних високошвидкісних верстатах з ЧПК за одновимірним рішенням при $H > 4$ на основі комп'ютерних підсистем проектування, контролю та діагностики операції шліфування.

Ключові слова: температура шліфування; температурні моделі; безрозмірна температура; рухливий джерело тепла; розподіл температури; форма теплового джерела; число Пекле

DOI: https://doi.org/10.15276/aait.03.2019.4
УДК 004.942:621.923

ТЕМПЕРАТУРНЫЕ МОДЕЛИ ДЛЯ МОНИТОРИНГА СОСТОЯНИЯ ТЕХНОЛОГИЧЕСКОЙ СИСТЕМЫ ШЛИФОВАНИЯ

Наталя Володимирівна Ліщенко[1)]
ORCID: https://orcid.org/ 0000-0002-4110-1321;odeslnv@gmail.com
Василь Петрович Ларшин[2)]
ORCID: https://orcid.org/0000-0001-7536-3859; vasilylarshin@gmail.com
[1)] Одесская национальная академия пищевых технологий, ул. Канатная, 112. Одесса, 65039, Украина
[2)] Одесский национальный политехнический университет, пр. Шевченко, 1. Одесса, 65044, Украина

АННОТАЦИЯ

Температура шлифования ограничивает производительность этой операции и является важным параметром для оценки состояния технологической системы. Однако в существующих компьютерных системах мониторинга и технологической

диагностики на станках с ЧПУ информация о текущей температуре шлифования отсутствует. Это вызвано трудностями прямого и косвенного измерения этого параметра. В первом случае – трудностями с установкой датчиков температуры, во втором – отсутствуют приемлемые математические модели для определения температуры шлифования. Цель исследования – разработка более простой температурной модели, приемлемой для современного шлифования с большими значениями скорости заготовки относительно шлифовального круга. Для достижения цели исследования была выполнена классификация решений трех-, двух- и одномерного дифференциальных уравнений теплопроводности с одинаковыми начальными и граничными условиями для исследования температур шлифования с помощью этих решений при прочих равных условиях. Условия близкого согласования результатов решений устанавливаются в зависимости от геометрической конфигурации зоны контакта между шлифовальным кругом и заготовкой: $H / L < 1$ и $H > 4$, где H и L - половина ширины и половина длины зоны контакта, соответственно. Вышеупомянутые три решения дифференциальных уравнений теплопроводности получены при граничных условиях второго рода и были преобразованы в однородную безразмерную форму, в которой безразмерная температура зависит от координаты и кратности безразмерного времени числу Пекле, которое характеризует это время, а также безразмерные полуширину и скорость движущегося источника тепла. Сравнительный анализ поверхностных и глубинных температур был выполнен для трех указанных выше решений в зависимости от числа Пекле. Показана возможность определения температуры шлифования на современных высокоскоростных станках с ЧПУ по одномерному решению при $H > 4$ на основе компьютерных подсистем проектирования, контроля и диагностики операции шлифования.

Ключевые слова: температура шлифования; температурные модели; безразмерная температура; подвижный источник тепла; распределение температуры; форма теплового источника; число Пекле

ABOUT THE AUTHORS

Natalia V. Lishchenko – PhD (Eng) (2006), Dr. Sci. (Eng) (2018), Dean of Faculty of Computer Science and Automation, Professor of the Department of Electromechanics, Mechatronics and Engineering Graphics. Odessa National Academy of Food Technologies, 112, Kanatna Str. Odesa, 65039, Ukraine

ORCID: https://orcid.org/0000-0002-4110-1321; odeslnv@gmail.com.
Research field: Information Support of Technological Processes

Наталя Володимирівна Ліщенко – кандидат технічних наук (2006), доктор технічних наук (2018), декан факультету Комп'ютерних систем та автоматизації, професор кафедри Електромеханіки, мехатроніки та інженерної графіки. Одеська національна академія харчових технологій, вул. Канатна, 112. Одеса, 65039,Україна

Vasily Petrovich Larshin – PhD (Eng) (1980), Dr. Sci. (Eng) (1995), Academician of the Ukrainian Academy of Economic Cybernetics (2020). Professor of Department of Mechanical Engineering Technology. Odessa National Polytechnic University, 1, Shevchenko Ave. Odesa, 65044, Ukraine
ORCID: https://orcid.org/0000-0001-7536-3859; vasilylarshin@gmail.com.
***Research field*:** Production and Technological Processes Information Ensuring

Василь Петрович Ларшин – кандидат технічних наук (1980), доктор технічних наук (1995), академік Української академії економічної кібернетики (2020), професор кафедри Технології машинобудування. Одеський національний політехнічний університет, пр. Шевченка, 1. Одеса, 65044, Україна